J|A|C|S
ARTICLES
Published on Web 06/18/2004

Structure and Reactivity of Ru Nanoparticles Supported on Modified Graphite Surfaces: A Study of the Model Catalysts for Ammonia Synthesis

Zhen Song, Tanhong Cai, Jonathan C. Hanson, Jose A. Rodriguez, and Jan Hrbek*

Contribution from the Chemistry Department, Brookhaven National Laboratory, Upton, New York 11973

Received December 15, 2003; E-mail: hrbek@bnl.gov

Abstract: Supported ruthenium metal catalysts have higher activity than traditional iron-based catalysts used industrially for ammonia synthesis. A study of a model Ru/C catalyst was carried out to advance the understanding of structure and reactivity correlations in this structure-sensitive reaction where dinitrogen dissociation is the rate-limiting step. Ru particles were grown by chemical vapor deposition (CVD) via a $Ru_3(CO)_{12}$ precursor on a highly oriented pyrolytic graphite (HOPG) surface modified with one-atomic-layer-deep holes mimicking activated carbon support. Scanning tunneling microscopy (STM) has been used to investigate the growth, structure, and morphology of the Ru particles. Thermal desorption of dissociatively adsorbed nitrogen has been used to evaluate the reactivity of the Ru/HOPG model catalysts. Two different Ru particle structures with different reactivities to N_2 dissociation have been identified. The initial sticking coefficient for N_2 dissociative adsorption on the Ru/HOPG model catalysts is $\sim 10^{-6}$, 4 orders larger compared to that of Ru single-crystal surfaces.

Introduction

Ru catalysts have shown much higher activity at lower temperatures and pressures in ammonia synthesis than the conventional iron catalyst, and they are becoming the next generation catalysts for ammonia synthesis.[1−4] Studies of this class of catalysts include: (1) the determination of the active site on Ru for N_2 dissociation, known to be the step-limiting process in ammonia synthesis, (2) the optimization of the Ru structure for the best activity, and (3) the search of a good support for Ru. It has been found that the nature of the supports influences greatly the Ru catalytic activity and that carbon is the most active among many of supports investigated thus far, including oxides, nitrides, zeolites, etc.[5−7] Although carbon-supported Ru catalyst has been used industrially in the ammonia synthesis process,[2] the stability of the carbon support is still a problem for the limited lifetime of the catalyst.[3] To find a more efficient and stable Ru catalyst, it is necessary to understand why the activity of the Ru/C system is superior to others and what factors control the catalyst stability.

The function of a support in a catalyst performance is one of the important issues in catalysis. The support can influence the catalytic activity by modifying the electronic properties of the active particles and by affecting the growth and ultimately the structure and morphology of the active particles that change the abundance of the active sites of the catalyst. Specifically, in the case of the Ru/C system, it has been found that the graphitization and texture of a carbon support are two crucial factors influencing the activity of the catalyst.[8−10] It is known that the texture of a substrate plays an important role in controlling the dispersion of the supported particles. Liang et al.[8] studied different carbon-supported Ru catalysts toward the ammonia synthesis reaction and found that catalytic activities in terms of turnover frequencies have the same trend as the electrical conductivities of the carbon support, a parameter indicating the extent of graphitization of the C materials. It has also been found that very high temperature (up to 1900 °C) treatment of a carbon support is needed before loading Ru to achieve a good activity of the catalysts.[8−10] Such a high temperature treatment basically induces a significant graphitization of the carbon material. However, no explanation of the correlations between graphitization and reactivity has yet been reported.

Among the reactions involved in ammonia synthesis, N_2 dissociative adsorption on the catalyst surface is the rate-determining step.[11] It has been shown that the active site for N_2 dissociation is the so-called B_5 site, made of five Ru atoms:

(1) Kowalczyk, Z.; Jodzis, S.; Raróg, W.; Zieliński, J.; Pielaszek, J.; Presz, A. *Appl. Catal., A* **1999**, *184*, 95.
(2) Bielawa, H.; Hinrichsen, O.; Birkner, A.; Muhler, M. *Angew. Chem., Int. Ed.* **2001**, *40*, 1061.
(3) Kowalczyk, Z.; Jodzis, S.; Raróg, W.; Zieliński, J.; Pielaszek, J. *Appl. Catal., A* **1998**, *173*, 153.
(4) Schlögl, R. *Angew. Chem., Int. Ed.* **2003**, *42*, 2004.
(5) Szmigiel, D.; Bielawa, H.; Kurtz, M.; Hinrichsen, O.; Muhler, M.; Raróg, W.; Jodzis, S.; Kowalczyk, Z.; Znak, L.; Zieliński, J. *J. Catal.* **2002**, *205*, 205.
(6) Hansen, T. W.; Hansen, P. L.; Dahl, S.; Jacobsen, C. J. H. *Catal. Lett.* **2002**, *84*, 7.
(7) McClaine, B. C.; Siporin, S. E.; Davis, R. J. *J. Phys. Chem. B* **2001**, *105*, 7525.
(8) Liang, C.; Wei, Z.; Xin, Q.; Li, C. *Appl. Catal., A* **2001**, *208*, 193.
(9) Raróg-Pilecka, W.; Szmigiel, D.; Komornicki, A.; Zieliński, J.; Kowalczyk, Z. *Carbon* **2003**, *41*, 579.
(10) Raróg, W.; Kowalczyk, Z.; Sentek, J.; Skladanowski, D.; Zieliński, J. *Catal. Lett.* **2000**, *68*, 163.
(11) Hinrichsen, O. *Catal. Today* **1999**, *53*, 177.

10.1021/ja031718s CCC: $27.50

two at step edges and three at the lower terraces.[12,13] Theoretical calculations and experiments have shown that the rate of N_2 dissociation is completely dominated by the steps.[12] Therefore, the ammonia synthesis reaction is extremely structure-sensitive on Ru. A marble model calculation showed that for round-shaped Ru particles, the abundance of B_5 sites had a sharp maximum at the particle size around 2.0 nm in diameter.[13] However, it was found experimentally that the NH_3 synthesis activity of the Ru catalysts increased with the size of Ru particles up to 5 nm in diameter and then became constant with the additional increase.[8,9] A better understanding of the particle size-dependent reactivity of the Ru catalysts requires the knowledge of the structure and morphology of the Ru particles with atomic resolution, especially that of the steps on the particle surfaces.

Transmission electron microscopy (TEM) studies of Ru particles grown on various supports, such as C, BN, Si_3N_4, MgO, $MgAl_2O_4$, and TiO_2, showed that in most cases Ru appears as round particles.[13−15] Some of the TEM images showed clearly orientational growths of Ru crystals relative to the support, e.g., Ru/SiN_4, Ru/BN, and Ru/TiO_2.[13−15] However, no evidence has been found for the orientational/epitaxial growth of Ru on graphite samples, probably because of the use of poorly crystallized graphitic supports.[13] Since a TEM image is a projection image, no detail information about the steps at the particle surfaces has been provided.

In this article, we present a scanning tunneling microscopy (STM) study of the growth of Ru particles on a highly oriented pyrolytic graphite surface by chemical vapor deposition via a $Ru_3(CO)_{12}$ precursor. To simulate the structure of activated carbon, we etched the surface with oxygen to form randomly distributed, one-atomic-layer-deep nanoholes on the surface. Unlike a TEM image, an STM image provides a three-dimensional structure of the Ru particles grown on the highly oriented pyrolytic graphite (HOPG) surface, especially the step structure on the surfaces of Ru particles, which is related closely to the reactivity of the catalyst. Our results have shown that a well-ordered, stepped graphite surface is crucial for the epitaxial growth of Ru particles. Ru grows laterally at the steps or hole edges of the HOPG surface and forms layered nanocrystals with the (0001) surfaces parallel to the graphite surface. The texture of the hole-modified HOPG surface plays a role in controlling the size and shape of the Ru particles. Reactivity study of the Ru/HOPG toward N_2 dissociation by using temperature-programmed desorption (TPD) shows a high efficiency of the dissociation of N_2 on the layered/stepped Ru nanocrystals. These results help to understand the importance of graphitization and texture of the carbon support for the preparation of Ru/C catalysts and point to a favorable Ru structure with a high activity for the ammonia synthesis process.

Experimental Section

Our preliminary experiments showed that $Ru_3(CO)_{12}$ sticks only on step edges of the HOPG surface. To obtain an evenly Ru-decorated surface, we first prepared a modified HOPG surface with randomly distributed one-atomic-layer-deep holes on the HOPG surface. A freshly cleaved HOPG sample was ion-sputtered in a UHV chamber with the 100 eV Ne^+ for ∼15−60 s. Then, the sample was oxidized in air at a temperature of 530 °C for ∼10−20min. Figure 1 shows two modified HOPG surfaces with one-layer-deep holes of 7 and 32 nm in diameter, respectively. The holes on the HOPG surfaces were generated by etching of the top graphite layer around the defect sites created by the ion sputtering. The density and the size of the holes could be adjusted by the time for sputtering and oxidation, respectively. In this way, we could control the texture of the HOPG surface.

Before the deposition of Ru, the HOPG sample was heated to 900 K in UHV for 1 h to remove the impurities (such as O_2, H_2O, CO, etc.) from the surface. We deposited Ru on the modified HOPG surface at 550 K by CVD via a $Ru_3(CO)_{12}$ precursor in a preparation chamber, which was separated from the STM chamber by a gate valve. The $Ru_3(CO)_{12}$ was kept in a glass vial at room temperature and connected with the preparation chamber with a gate valve.[16] The exposure of Ru carbonyl was controlled by dosing time, and the surface concentration of Ru was determined by Auger electron spectroscopy (AES) using the published Auger data.[17] This approach can lead to errors of factor of 2 in surface concentration determination.[18] Since the strongest AES peaks of Ru and C overlap at 272−273 eV, the Ru concentration was calculated using the Ru 231 eV peak together with the mixed peak at 272 to 273 eV. The fraction of surface covered by Ru particles was also measured independently from STM images.

After the preparation, the samples were transferred under vacuum to the STM chamber (Omicron, base pressure $\sim 5 \times 10^{-11}$ Torr). The STM measurements were performed at room temperature with a tungsten tip.

N_2 dissociation on the Ru/HOPG was studied by TPD in a separate UHV chamber (base pressure $\sim 4 \times 10^{-10}$ Torr) equipped with a high-pressure cell. N_2 adsorption could be carried out in either the main chamber or the high-pressure cell. In the main chamber we used a tube doser with the enhancement factor[19] of ∼3 for dosing nitrogen. The effect of the hot filament of the ion gauge on the probability for dinitrogen dissociative chemisorption in our chamber was much less than previously reported.[20] With the sample mounted 0.6 m away and out of the direct line-of-sight from the ion gauge, we measured a 2-fold increase in nitrogen surface concentration with the filament switched on during N_2 exposure. The high-pressure cell, isolated from the main chamber by a gate valve, allowed the adsorption of N_2 at pressures up to 1 atm and the direct transfer of the sample to the main chamber for the TPD measurement after evacuation. The modified HOPG substrates were characterized by STM before installation into the TPD chamber. The thermocouple was cemented to the back of the sample. TPD spectra were recorded with a heating rate of 2 K/s. High purity $^{14}N_2$ (99.999%) and isotope $^{15}N_2$ gases were used as received. Since both N_2 and CO have mass spectrum of parent species at $m/e = 28$, we monitored nitrogen signal at fragment with $m/e = 14$ where $^{14}N^+$ represented 14% of the N_2^+ intensity, while CO^{2+} fragment was only 0.8% of the parent CO^+ signal (for a more detailed discussion, see ref 20).

Some of the Ru/HOPG samples used in the TPD study were first measured by STM and then transferred through air to the TPD chamber; the others were directly prepared in the TPD chamber. The samples transferred through air were reduced by H_2 in the TPD chamber until no O_2 was detected by AES.

Results and Discussions

Structure of the Ru/HOPG Model Catalyst. Figures 2 and 3 show the STM images and analysis of Ru deposited on the

(12) Dahl, S.; Logadottir, A.; Egeberg, R. C.; Larsen, J. H.; Chorkendorff, I.; Törnqvist, E.; Nørskov, J. K. *Phys. Rev. Lett.* **1999**, *83*, 1814.
(13) Jacobsen, C. J. H.; Dahl, S.; Hansen, P. L.; Törnqvist, E.; Jensen, L.; Topsøe, H.; Prip, D. V.; Møenshaug, P. B.; Chorkendorff, I. *J. Mol. Catal. A* **2000**, *163*, 19.
(14) Hansen, T. W.; Wagner, J. B.; Hansen, P. L.; Dahl, S.; Topsøe, H.; Jacobsen, C. J. H. *Science* **2001**, *294*, 1508.
(15) Komaya, T.; Bell, A. T.; Weng-Sieh, Z.; Gronsky, R.; Engelke, F.; King, T. S.; Pruski, M. *J. Catal.* **1994**, *149*, 142.
(16) Cai, T.; Song, Z.; Chang, Z.; Liu, G.; Rodriguez, J. A.; Hrbek, J. *Surf. Sci.* **2003**, *538*, 76.
(17) Davis L. E.; MacDonald, M. C.; Palmberg, P. W.; Riach, G. E.; Weber, R. E. *Handbook of Auger Electron Spectroscopy*, 2nd ed.; Physical Electronics Inc.: Eden Prairie, MN, 1976.
(18) Woodruff, D. P.; Delchar, T. A. *Modern Techniques of Surface Science*; Cambridge University Press: Cambridge, 1988; p 146.
(19) Campbell, C. T.; Valone, S. M. *J. Vac. Sci. Technol., A* **1985**, *3*, 408.

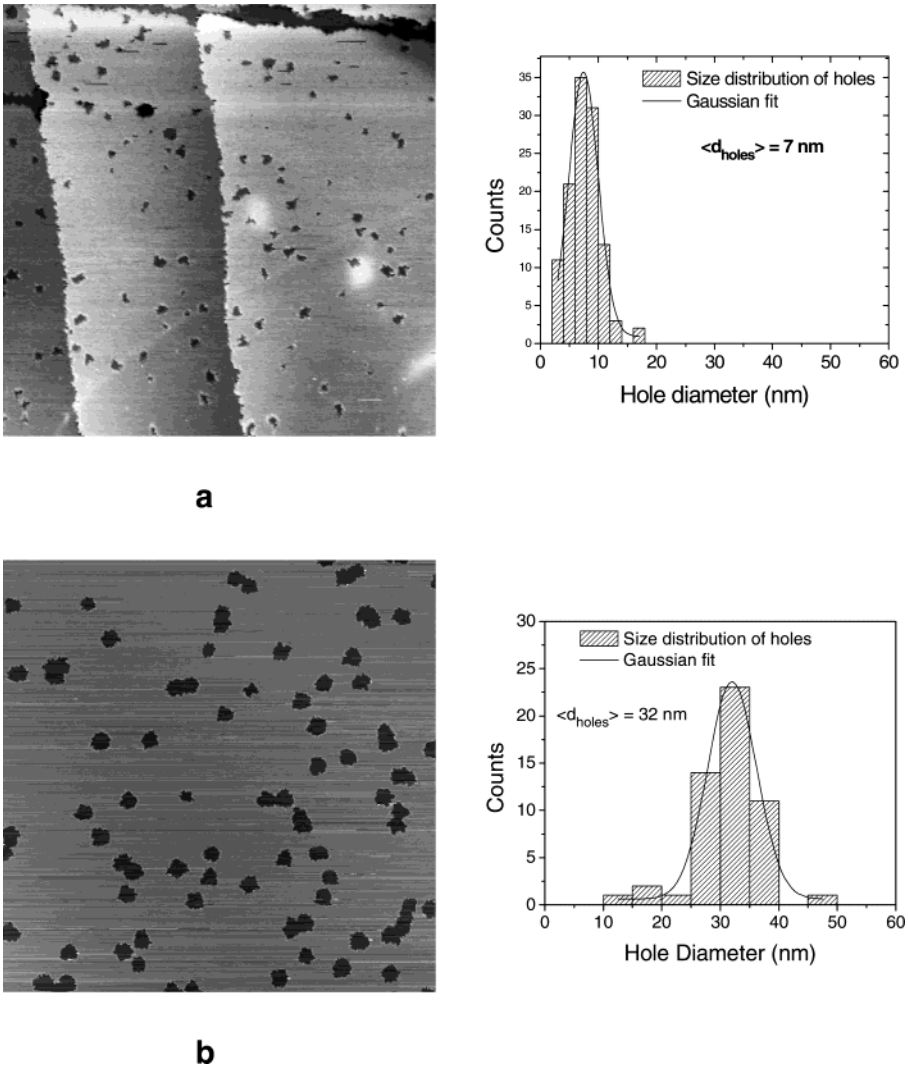

Figure 1. STM images of two HOPG surfaces modified by one-atomic-layer-deep holes with diameters of (a) 7 and (b) 32 nm. Image size: (a) 400 × 400 nm^2 and (b) 800 × 800 nm^2.

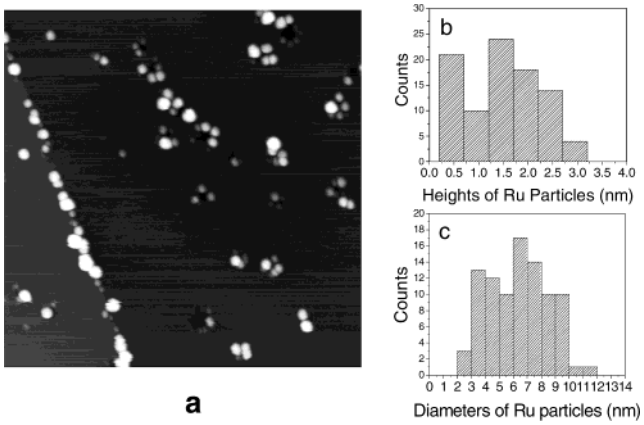

Figure 2. (a) STM image of a small hole-modified Ru/HOPG surface (2 atom % Ru). Image size: 200 × 200 nm^2. (b) Height and (c) diameter distributions of the Ru particles in (a).

small hole-modified HOPG surface displayed in Figure 1a at two Ru coverages. The corresponding AES spectra are shown in Figure 4, together with a clean HOPG AES spectrum. The Ru dosing time is 20 min for the first sample and another 25 min for the second sample. No oxygen is detected by AES at either of the Ru coverages, indicating that the $Ru_3(CO)_{12}$ has completely decomposed and that the deposited Ru is in metallic state. XANES and XRD measurements (not shown) corroborated the formation of metallic Ru on HOPG.

Figure 2a shows that the growth of Ru starts from the step edges and the edges of holes of the modified HOPG substrate. The Ru particles appear as round islands. The apparent height distribution is shown in Figure 2b, displaying two maxima at ~0.5 and ~1.5 nm, respectively. Similarly, the apparent diameter distribution of the particles shows also two peaks at ~3.5 and ~6.5 nm, respectively (Figure 2c), indicating a bimodal growth of Ru on the HOPG surface. Our previous studies on the CVD growths of Mo and Ru on a Au(111) surface have shown that the nucleation of metal clusters occurred before their anchoring on the surface.[16,21] The bimodal CVD growth of Ru on HOPG may proceed by the nucleation of Ru during the $Ru_3(CO)_{12}$ decomposition to form small particles and by the sintering of the small particles to big ones. The Ru surface concentration of this sample measured by AES is ~2 atom %,

(20) Dietrich, H.; Geng, P.; Jacobi, K.; Ertl, G. *J. Chem. Phys.* **1996**, *104*, 375.

(21) Song, Z.; Cai, T.; Rodriguez, J. A.; Hrbek, J.; Chan, A.; Friend, C. *J. Phys. Chem. B* **2003**, *107*, 1036.

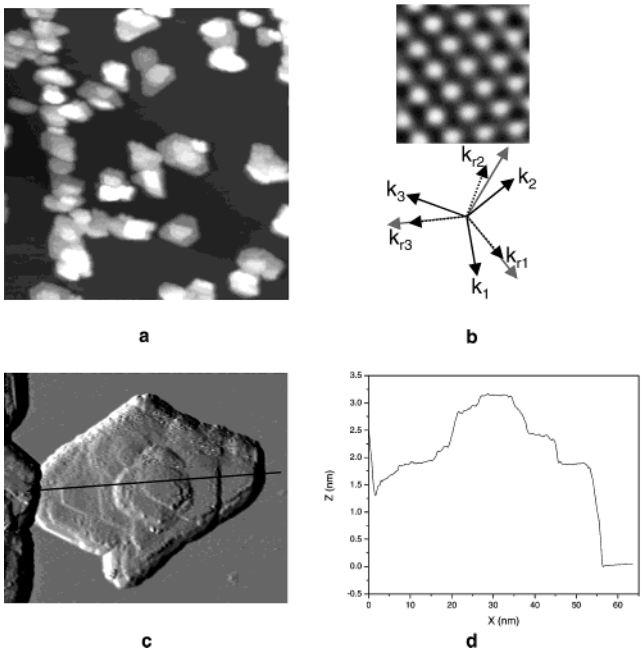

Figure 3. (a) STM image of a small hole-modified Ru/HOPG surface (30 atom % Ru). Ru forms flat, layered particles that completely cover the holes. Image size: 200 × 200 nm^2. (b) The orientations of the steps of the Ru particles (black and dotted arrows) shown in (a), and the HOPG lattice orientation (gray arrows) obtained from an atomic resolution STM image shown. Image size: 1.1 × 1.1 nm^2. The gray arrows are rotated by 30° from the hexagonal atomic structure of the HOPG surface because the STM displays every other C atom of the graphite surface.[29] (c) A close-up differential image of a Ru particle. Image size: 70 × 55 nm^2. (d) A line profile across the Ru particle shown in (c).

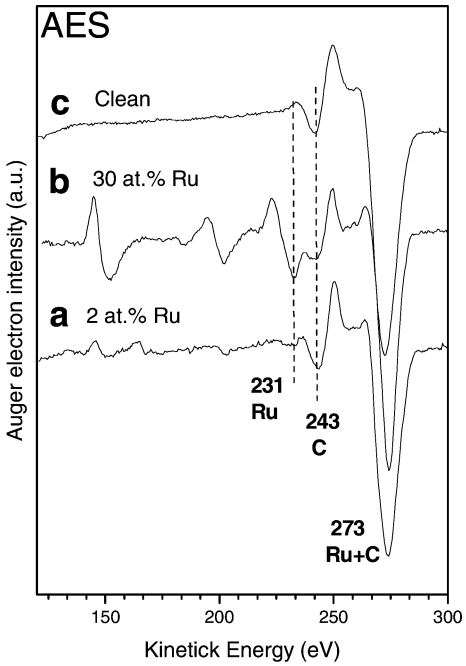

Figure 4. AES spectra of the samples shown in Figure 2 (spectrum a) and Figure 3 (spectrum b). Spectrum c is from a clean HOPG sample.

while the Ru covered area fraction obtained from STM images is ∼7%. The disagreement can be caused by the STM tip convolution that overestimates the Ru particle diameters; on the other hand, a contribution of the carbon AES signal under the Ru particles leads to a lower estimate of the Ru surface concentration by AES.

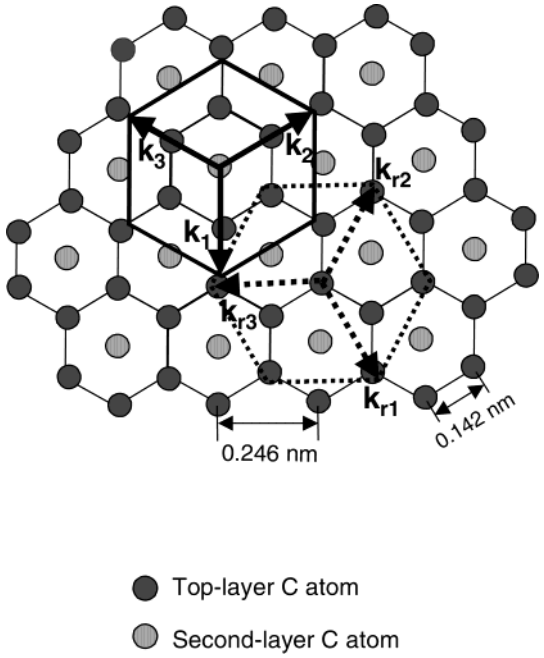

Figure 5. Two possible epitaxial growths of Ru on a HOPG surface, denoted by the large hexagons with the sides equal to the Ru lattice constant (0.271 nm). The two Ru lattices are rotated relatively by 30°. The small circles represent the carbon atoms at the top (dark gray) and the second (light gray) layers of the graphite surface.

Figure 3a is an STM image of a higher Ru surface concentration, ∼30 atom % (AES measurement), on the same HOPG surface. The apparent Ru area fraction measured by STM is 36%. At this Ru coverage, the etched holes on HOPG have been completely covered by the Ru particles. STM images show that the Ru particles have layered structure with the steps on the particles running along six directions (Figure 3b). Figure 3c is a close-up image of one Ru particle, displaying the layered crystalline structure. A line profile across the crystal is shown in Figure 3d. The highest part of the particle reaches ∼3 nm, and the width is ∼ 50 nm. On average, the height of the Ru particles in Figure 3a have increased by a factor of ∼3, and the apparent coverage increased by a factor of ∼18, compared to those in Figure 2a. This indicates that Ru grows much faster laterally than vertically.

Many of the Ru islands show regular triangular or truncated triangular shapes derived from hexagonal structures, implying a (0001) surface orientation. The single step height on the Ru particles is 0.22 ± 0.03 nm, consistent with the step height (0.214 nm) on a Ru (0001) surface. The six side orientations of the Ru crystals, shown in Figure 3b, can be treated as two sets of threefold symmetry axes, relatively rotated by 30° around the surface normal. One set is coincident with the orientation of the atomic resolution image of HOPG surface (Figure 3b). The small angle deviations arise from the drift of the microscope.

On the basis of these results, we propose that the growth of Ru on a graphite surface is epitaxial and has two orientations, both with the (0001) surfaces parallel to the graphite (0001) surface. One of them has the same orientation as the HOPG hexagonal lattice (indicated by k_1, k_2, and k_3 vectors); the other is 30° rotated around the surface normal, indicated by k_{r1}, k_{r2}, and k_{r3} (see Figure 5). Considering that the nearest-neighbor atom distance of the Ru(0001) surface is 0.271 nm, and that of the HOPG surface is 0.142 nm, the mismatches of the Ru (0001)

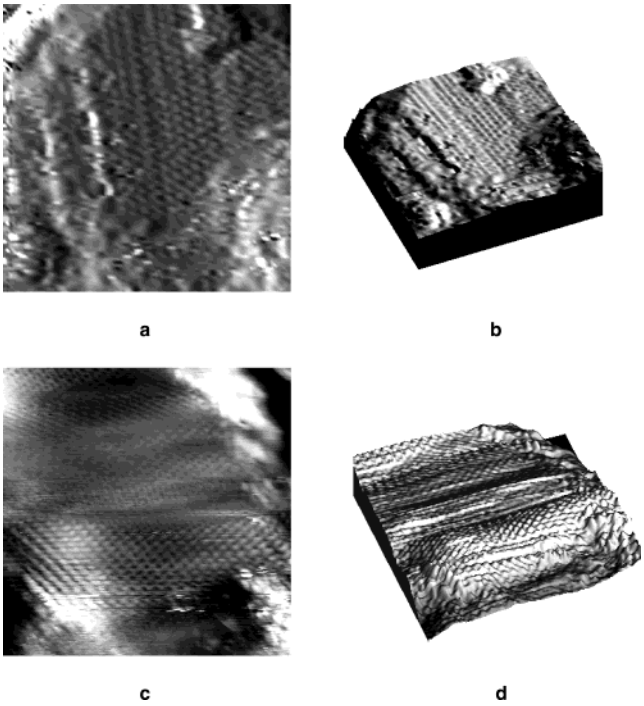

Figure 6. Atomic resolution images (10×10 nm^2) of two Ru particles with different orientations. (a), (c) Top view and (b), (d) three-dimensional images.

lattice (shown as the big hexagons in Figure 5) to the two corresponding hexagonal structures derived from the HOPG lattice are -4.7% and $+9.8\%$, respectively.

The atomic resolution STM images of the Ru crystals, shown in Figure 6a and c, directly prove this interpretation. Both images show that the surface atoms of Ru are arranged in hexagonal structure, indicating the (0001) surface. The selected two crystals are rotated 30° to each other. The crystal shown in Figure 6c has the same orientation as that of the HOPG substrate.

Parts a and b of Figure 7 are STM images of an as-deposited Ru (14 atom %)/HOPG surface that was modified with large holes (Figure 1b). The Ru particles start to grow at the step or hole edges of the HOPG surface. Some of the large Ru particles have formed by aggregation of small particles. Figure 7c,d shows images of the sample after annealing to 800 K, which has resulted in further aggregation and better crystallization of the Ru particles. Unlike the growth on small holes, Ru particles growing on the large hole-modified HOPG surface have an elongated shape. Two different Ru orientations rotated by 30° are also found on this sample, shown by Figure 7e. The edge angles of the particles imply a (0001) surface orientation. Figure 7c,d also shows that the Ru crystallites grown on the area with higher density of the holes are smaller and that the big Ru crystals are usually found at large extended graphite surface areas.

The reason for the formation of elongated shape particles is unknown. One possibility is that an asymmetric electric field is present around a particle at an edge of a large hole due to the broken symmetry at the edge. This electric field could influence the state and diffusion of the $Ru_3(CO)_{12}$ molecules and fragments.[22] In the case of the small hole decorated surface, the holes are fully covered by Ru and the growing of particles are more symmetrical.

Stability of the Ru Particles upon Oxidation and Reduction. Ru catalysts can be oxidized by exposure to air, and they can be reduced to metallic state in the H_2. To test the stability of the Ru on HOPG during these processes, we oxidized and then reduced the Ru/HOPG sample that is shown in Figure 3a. The oxidation was carried out in O_2 of $\sim 2 \times 10^{-7}$ Torr at 800 K for 1 h, and the reduction was carried out in H_2 of $\sim 2 \times 10^{-5}$ Torr at 550 K for 2 h. The sample was then annealed to 800 K for 1 h. After the oxidation, oxygen was detected on the sample by AES (not shown), indicating the formation of ruthenium oxide. Meanwhile, the surface Ru concentration decreased to 15 atom %, a 50% loss from the original sample. This loss is most probably caused by the sublimation of ruthenium oxide during the oxidation at high temperature.[23] AES measurements also showed that the oxide was readily reduced by the H_2 treatment without further loss of Ru from the sample.

We tried to image the oxidized Ru sample by STM and found that it was impossible to obtain a stable image. The Ru particles were easily pushed away by the STM tip. This could be caused by the bond weakening between nanoparticles and the graphite substrate after the oxidation. After the reduction, the STM measurement again became possible. Figure 8a is an STM image of Ru/HOPG after the oxidation and reduction. The Ru particles still keep the flat shape, and the additional coalescence between particles has also occurred. The height distribution of the Ru particles on this sample is slightly broader than that of the as-deposited sample, as shown in Figure 8b. The average heights are 3.3 and 4.8 nm for the as-deposited Ru and that after the oxidation and reduction treatments, respectively.

Overall, a fraction of the Ru in the catalysts is lost as an oxide at higher temperatures. However, the morphology of the Ru particles on HOPG is stable, keeping the flat, layered form.

N_2 Dissociation on the Ru/HOPG Surfaces. Figure 9A shows that there is a large background desorption of nitrogen from HOPG. The N_2 TPD spectra from a clean modified HOPG surface after exposure to 2×10^{11} L (curve a) and 1×10^{11} L (curve c) of N_2 at room temperature were monitored with $m/e = 14$ to distinguish between CO and N_2 contributions. The featureless curve b in Figure 9A is a blank TPD of $m/e = 14$ spectrum recorded right after acquiring curve a without exposure to N_2. The broad desorption peak probably arises from the molecular N_2 adsorbed at the defect sites of HOPG and/or the subsurface N_2 formed by penetration of the N_2 molecules into the sublayer of the HOPG through the defect sites. We treat this broad desorption feature as a background signal and subtract it from the TPD curves as shown in Figure 9B, curves c and d. This background signal, found in all high-pressure adsorption experiments, is absent in the high-vacuum ones. Additionally, a small contribution (0.8%) from doubly ionized CO to the signal of $m/e = 14$ (Figure 9B, curve b) is also subtracted from the total $m/e = 14$ signal (Figure 9B, curve a). The final curve d is that of N_2 desorption signal from Ru particles. This data processing procedure is validated by an isotope experiment (see below).

Figure 10 shows representative TPD spectra from samples of different morphologies after the data processing described

(22) Pascual, J. I.; Jackiw, J. J.; Song, Z.; Weiss, P. S.; Conrad, H.; Rust, H.-P. *Phys. Rev. Lett.* **2001**, *86*, 1050.

(23) *CRC Handbook of Chemistry and Physics*, 46th ed.; Chemical Rubber Co.: Cleveland, Ohio, 1965−1966.

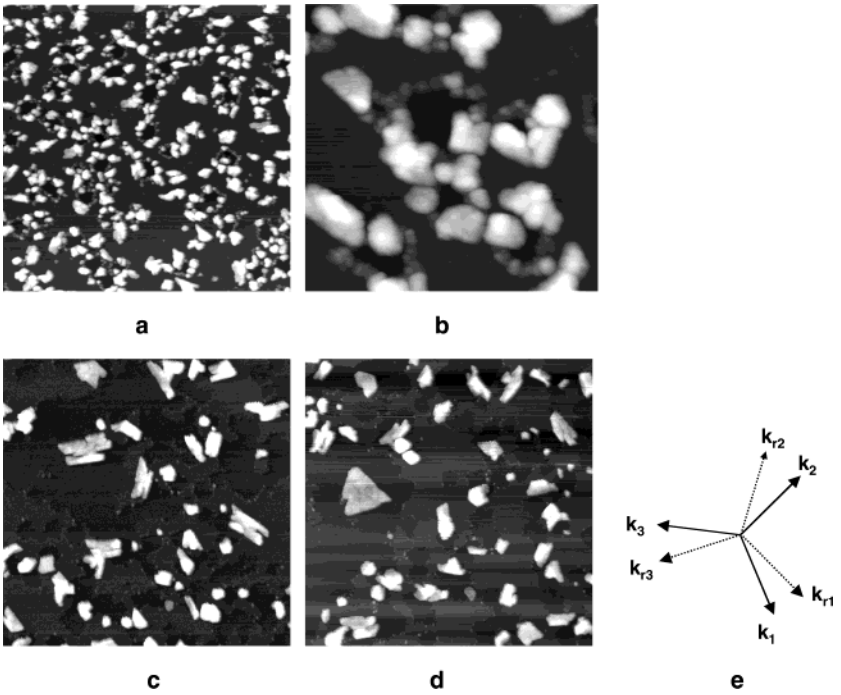

Figure 7. STM images of large hole-modified Ru/HOPG surface (~14 atom % Ru). (a), (b) As deposited. (c), (d) After annealing to 800 K. The image sizes: (a), (c), and (d) 400 × 400 nm^2, (b) 100 × 100 nm^2. (e) The Ru crystallites step orientations.

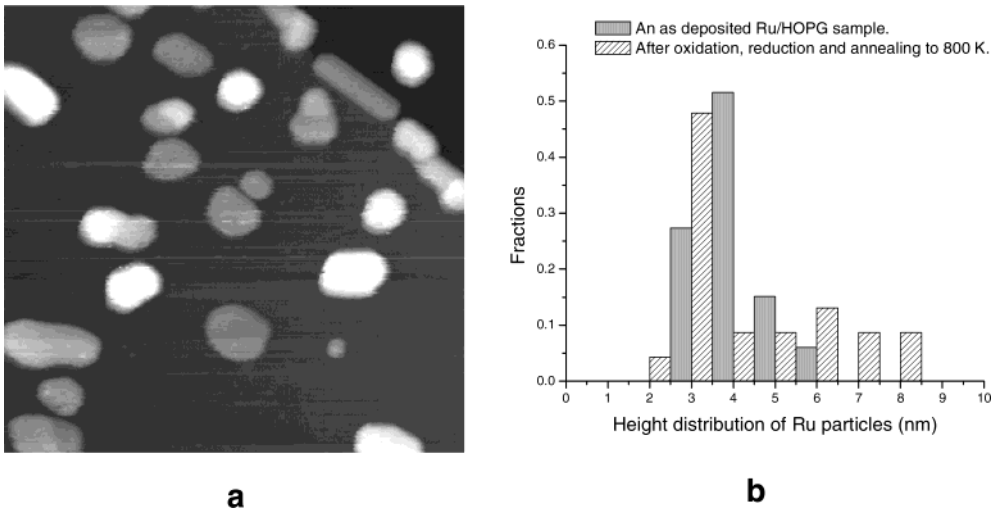

Figure 8. (a) STM image of the Ru/HOPG sample (15 atom % Ru) after the oxidation and reduction treatment. Image size: 200 × 200 nm^2. (b) The height distributions of the Ru/HOPG sample before and after the oxidation and reduction.

above. Curve a is a TPD spectrum of $^{15}N_2$ ($m/e = 30$) from a sample (Ru: ~15 atom %) with the large flat particles similar to that shown in Figure 3a after exposure to 6 × 10^4 L of $^{15}N_2$ at 400 K under high vacuum. The isotope experiment confirms that the peak at 520 K is due to the N_2 desorption. This experiment has been reproduced for several samples that have been measured by STM either before or after the TPD measurements. The morphologies of these samples are shown in Figures 3a, 7c and d, or 8a, in which the Ru particles expose flat, layered structure of the (0001) surface. The N_2 adsorption has been carried with both $^{14}N_2$ and $^{15}N_2$ at both low (~10^{-5} Torr) and high (~10 Torr, $^{14}N_2$ only) pressures. All the TPD spectra show a peak at ~500 K. At larger exposure, the peak position shifts to lower temperature as expected for the second-order desorption of N_2 formed by recombination of the atomic nitrogen on the surface.

Curve c is the N_2 TPD spectrum ($m/e = 14$) from a sample with ~2 atom % Ru of a small, round particles (similar to those shown in Figure 2a), after an exposure of 2 × 10^{11} L $^{14}N_2$ at 400 K. Small exposures of N_2 comparable to those for curves a and b did not result in detectable TPD peak on this sample. To allow direct comparison with curve a, curves b and c have been multiplied by 7, the parent/fragment ratio of N_2^+/N^+. The TPD spectrum c shows the N_2 desorption from the round particle peaks at 650 K.

Curve b is from a sample prepared exactly the same way as for the sample shown in Figure 7a,b. STM images have shown the modification holes on both samples are the same; AES spectra show the Ru surface concentrations are also identical. We, therefore, assume that the TPD curve b is from a sample with morphology imaged in Figure 7a, which shows both small round and large flat Ru particles. The N_2 adsorption was carried

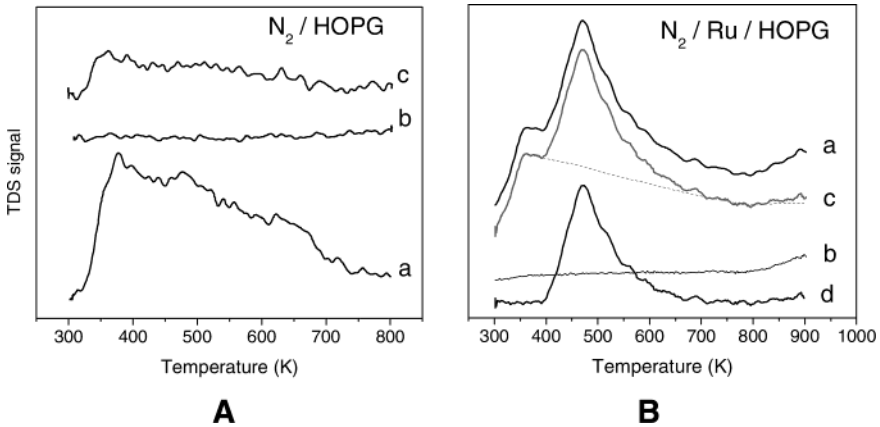

Figure 9. TPD spectra of N_2 ($m/e = 14$) from (A) clean HOPG surface and (B) Ru/HOPG surface. Panel (A): (a) 2×10^{11} L N_2 at 300 K, (b) no N_2 exposure, and (c) 1×10^{11} L N_2 at 300 K. Panel (B): simultaneous record of (a) $m/e = 14$ and (b) $m/e = 28$ (multiplied by 0.008) after 2×10^{10} L N_2 exposure at 300 K, (c) subtraction of (b) from (a), the dotted line represents a scaled contribution from a clean HOPG, and (d) subtraction of the dotted curve from (c).

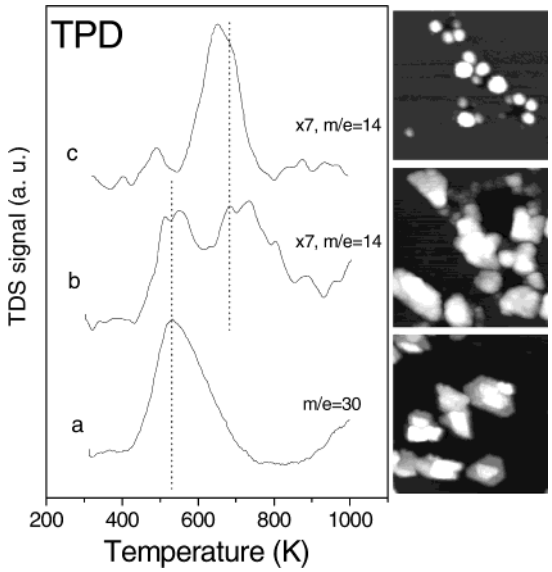

Figure 10. TPD spectra from (a) large flat Ru crystallites (~15 atom % Ru), 6×10^4 L $^{15}N_2$ at 400 K, (b) small, round and large, flat Ru particles (~14 atom % Ru), 3×10^4 L $^{14}N_2$ at 400 K, and (c) small, round Ru particles (~2 atom % Ru), 2×10^{11} L $^{14}N_2$ at 300 K. The STM images are the representative surface morphologies of the corresponding TPD curves.

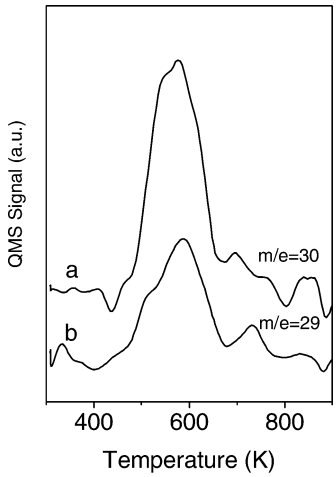

Figure 11. $^{15}N_2$ (a) and $^{15}N\,^{14}N$ (b) TPD spectra from a Ru/HOPG sample (~10 atom % Ru) first exposed to $^{15}N_2$ (2×10^5 L) and then to $^{14}N_2$ (4×10^4 L) at 400 K.

out in the main chamber of 4×10^{-6} Torr at the sample temperature of 400 K. Two TPD peaks have been observed, one at ~500 K, and the other at ~700 K. We suggest that the ~500 K peak in the curve b originates from the large flat Ru particles (see curve a) and that the 700 K peak (b) and the 650 K peak (c) have the same origin, namely the round Ru particles. The shift in the peak positions may arise partially from the N coverage difference due to the second-order desorption of N_2 and partially from the size difference of the particles on the surfaces. The small round particles on the as-deposited sample (b) have an apparent height of ~1 nm (Figure 7a,b), while the round Ru particles on the annealed sample (c) are taller (an apparent height of ~3 nm), as measured by STM after the TPD experiment.

Figure 11 shows the isotope exchange experiment. The Ru/HOPG sample (400 K) was first exposed to $^{15}N_2$ (2×10^5 L), and then the dosing gas was switched to $^{14}N_2$ (2×10^4 L). Signals from $m/e = 30$ and 29 were recorded for the TPD spectra. Since $^{14}N^{15}N$ ($m/e = 29$) can only be obtained by recombination of ^{14}N and ^{15}N atoms on the Ru surfaces, this experiment verified dissociative adsorption of N_2 on the Ru particle surface.

Figure 12 shows two TPD spectra from the same sample after two different exposures to N_2. The lower exposure curve (the same one shown in Figure 10b) is from an as-deposited sample, and we used it to calculate the N_2 dissociative adsorption probability, which is assumed to be close to the initial sticking coefficient s_0. The amount of adsorbed N is determined by comparing the peak area of the N_2 TPD curve with that of CO saturated adsorbed on a Ru (0001) surface at room temperature, where $\theta_{CO} = 0.6$.[24] Interestingly, the sticking coefficient of N_2 on the Ru/HOPG system is $\sim 1 \times 10^{-6}$, 4 orders larger than that on a Ru (0001) single-crystal surface (9×10^{-11}) measured by Dahl et al. at 400 K.[25] Although at low coverage the N concentrations on the two different structures of the Ru particles are nearly the same, N coverage on the flat particles increased much more than that on the round particles. Additionally, the desorption peak from the round Ru particles shifts significantly (from 710 to 620 K), more than expected for the coverage dependence of N_2 desorption. A structural change of these

(24) Pfnür, H.; Feulner, P.; Menzel, D. *J. Chem. Phys.* **1983**, *79*, 4613.
(25) Dahl, S.; Törnqvist, E.; Chorkendorff, I. *J. Catal.* **2000**, *192*, 381.

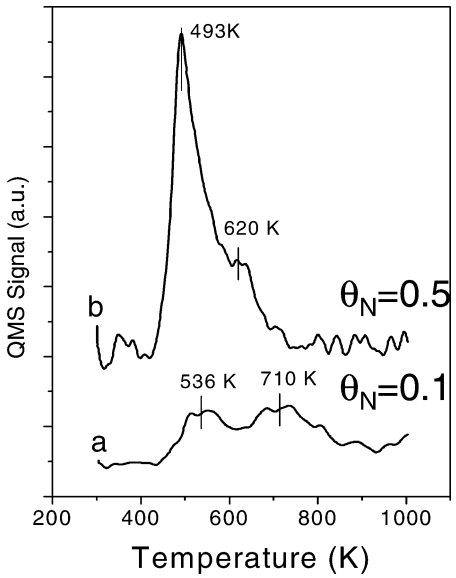

Figure 12. TPD spectra of N_2 at $m/e = 14$ from a Ru/HOPG sample (~14 atom % Ru) after exposure to N_2 of (a) 3×10^4 L and (b) 2×10^{10} L at 400 K.

particles must have occurred during the temperature ramping of the TPD experiments. STM images (Figure 7) have shown the sintering of the Ru particles upon annealing. Since the Ru particles with the flat, layered structure are more stable and have larger capacity for atomic N, they may have an ideal structure and morphology required for the ammonia synthesis.

After several rounds of TPD experiments, the activity of the catalyst decreases. One possible explanation is that the active sites on Ru are poisoned by carbon coming from the CO impurity in the N_2 gas and from the graphite substrate. We have found that oxidation and reduction treatment can reactivate the Ru/HOPG catalyst. The reactivated sample shows the same TPD features as those presented in Figure 10a,c.

In conclusion, we suggest that the TPD peak at ~650 K is from small, round Ru particles, and the peak at ~500 K is from large flat Ru particles. The broad desorption feature starting at ~380 K is from adsorption of N_2 at defect sites of the HOPG surface during high-pressure exposures.

Reactivity and Structures. Diekhöner et al.[26] reported TPD of N_2 from a Ru(0001) single-crystal surface after exposing Ru(0001) to an atomic beam of N. They found that at low coverage ($\Theta_N \approx 0.3$), desorption of N_2 occurs at ~800 K, consistent with that obtained by adsorbing N_2 on Ru(0001).[25] With the increase of the N coverage, weakly bonded species formed on the surface and desorbed at temperature between ~400−600 K. Specifically, when the N coverage was larger than 0.5, the low-temperature desorption (centered at 500 K) dominated the TD spectrum. However, by exposing the Ru(0001) single-crystal surface to N_2, the N coverage is always less than 0.3;[25] there has been no report of the low-temperature desorption. It is interesting that the N_2 desorption peak from the flat, layered Ru particles in our experiment appears at ~500 K. This could imply a fact that the N_2 dissociation rate on the Ru/HOPG is high and allows the formation of high N coverage on the flat Ru particles. The observed N coverage of ~0.5 on Ru/HOPG confirms this deduction.

The high dissociation rate of N_2 on Ru/HOPG can be ascribed to the high density of steps on the particle surfaces. Besides this, our STM images (Figure 6b,d) show that the surfaces of the Ru particles are not perfectly flat. This implies the presence of dislocations within the Ru particles and on their surfaces and, consequently, induction of surface strain. Wintterlin et al.[27] observed directly by STM that a stretched Ru(0001) surface was much more active to NO dissociation; the N coverage at the stretched part of the strained surface was much higher, while it was lower at the compressed part. Therefore, in our system, it is possible that the atomic N has higher concentration at certain strained areas on the Ru particle surfaces, which induces higher fraction of the low-temperature desorption peak of N_2.

Dietrich et al.[20,28] studied nitrogen TPD from opened surfaces of single-crystal Ru surfaces, $(10\bar{1}0)$ and $(11\bar{2}1)$, after exposure to N_2 gas. On these two surfaces, two and four layers of Ru atoms are exposed, respectively. The N_2 desorption from both surfaces are found at ~650 K. We can safely assume that a Ru particle with a round shape has larger fraction of opened surfaces than the one with a flat shape. The N_2 desorption peak at ~650 K found from small round particles could be due to the desorption from those opened surfaces.

Unlike the close-packed Ru(0001) surface, subsurface N can form on both of the opened surfaces, with the concentrations possibly 10 times more than that on the surface.[20,28] This difference shows an additional advantage of the (0001) surface, which can hold the N atoms at the surface for the further NH_3 synthesis reactions.

In summary, we assume that two major structural features can be related to the high activity in ammonia synthesis of the Ru/C system: (1) the well-ordered graphite substrate, corresponding to high extent of graphitization and (2) the layered and strained (0001) surfaces of the Ru particles. The former allows the lateral growth of Ru on graphite, and in this way the Ru surface area could be larger than that of ball-like particles. The latter results in a relatively high density of B_5 sites for N_2 dissociation, and the (0001) terraces serves as storage for the surface N atoms that migrated from the step edges after the dissociation. The strain on the surfaces of the flat Ru particles lowers the adsorption energy of N atoms, which could also contribute to the high activity of the catalyst.

Conclusions

We have manipulated the growth of Ru nanoparticles on a hole-modified HOPG surface and prepared two kinds of Ru clusters, round ones and flat, layered ones, by controlling the texture of the HOPG surface and the surface concentration of Ru. The growth of Ru on graphite is epitaxial. Two growth orientations have been found. Both have the (0001) surfaces parallel to the graphite surface. One has the same orientation as the graphite lattice; the other is 30° rotated around the surface normal. The texture of the graphite surface influences the size and shape of the Ru particles.

(26) Diekhöner, L.; Mortensen, H.; Baurichter, A.; Huntz, A. C. *J. Vac. Sci. Technol., A* **2000**, *18*, 1509.
(27) Wintterlin, J.; Zambelli, T.; Trost, J.; Greeley, J.; Mavrikakis, M. *Angew. Chem., Int. Ed* **2003**, *42*, 2850.
(28) Dietrich, H.; Jacobi, K.; Ertl, G. *J. Chem. Phys.* **1997**, *106*, 9313.
(29) Hembacher, S.; Giessibl, F. J.; Mannhart, J.; Quate, C. F. *Proc. Natl. Acad. Sci. U.S.A.* **2003**, *100*, 12539.

The N_2 adsoption/desorption behaviors on the round and flat Ru particles are different. N_2 that dissociates on round Ru particles partially diffuses to the bulk of Ru particles, and the part staying at surface desorbs at ~650 K. N_2 that dissociates on flat Ru particles forms a high density of atomic N on the (0001) terraces because of the large number of step sites and strained (0001) surface, and it desorbs at ~500 K. The possibility to form such a high density of atomic N on the surface may be the reason for the high activity of Ru/C catalysts in the NH_3 synthesis.

The extent of graphitization is important for the activity of the Ru/C catalyst. A well-ordered graphite surface directs the epitaxial growth of Ru and allows the formation of the flat, layered Ru crystals.

Acknowledgment. This research was supported by the U.S. Department of Energy, Division of Chemical Sciences, under Contract DE-AC02-98CH10886.

JA031718S